Table 1 Clinical and radiological findings in mesomelic dysplasia Kantaputra type

Characteristic findings	Ref. [1,4,5]	Ref. [3]	Ref. [2]	Reported patient
Short stature	Y	Y	Y	Y
Craniofacial dysmorphism	N	N	N	N
Delayed milestones	N	N	N	N
Normal karyotype	Y	Y	Y	Y
2q24-q32 linkage	Y	N	N	
Bilateral symmetric skeletal involvement	Y	Y	Y	Y
Wide distal humeral epiphysis	Y			Y
Short bowed broad radius	Y	Y	Y	Y
Short broad ulna	Y	Y	Y	Y
Ulna shorter than radius	Y	Y	Y	Y
Hand in ulnar deviation	Y	Y*	Y	Y
Carpal synostoses	Y*	N	Y	?
Carpal deficits	Y*	N	Y	?
Defects of metacarpals or phalanges	N	N	Y	N
Phalangeal joint contractures	Y	Y	Y	Y
Shortening of tibia and fibula	Y	Y	Y	Y
Proximal fibular hypoplasia	Y	Y		Y
Prominence on distal fibula	Y	N	Y	N
Tarsal synostoses	Y*	N	Y	Y
Tarsal deficits		N	Y	?
Malformation of talus/ calcaneus	Y	Y	Y	Y
Bifid calcaneus				At early age
Defects of metatarsals/ phalanges	N	N	Y hallux valgus	N
Pes equinovarus	Y	Y	Y or pes cavus/ planus	Y
Tiptoe gait	Y	N-early surgical correction		Y[b]
Delayed ossification	Y			Y
Other skeletal involvement	N	N	Scoliosis	N
Extraskeletal involvement	N	N	One sensori-neural hearing loss	N

*Not all patients.
[b]Before surgical correcion.
? Not determined because of young age.

More profound differential diagnosis is however necessary in distinguishing Kantaputra from Nievergelt and Langer type. Langer type is a homozygous state of a less severe pseudoautosomal dominant Leri–Weill dyschondrosteosis [8] (a progressive Madelung deformity of the forearms and a mild-to-moderate short stature [7]). In Langer mesomelia, bilateral short and bowed radius, short hypoplastic ulna, and ulnarly deviated hand closely resemble that of Kantaputra. Moreover, there are rudimentary fibula, short tibia with talipes equinovarus, tiptoe gait, and delay in development of secondary ossification centers, primarily in ulna, fibula, and radius. Nevertheless, Kantaputra arises in a family as a new incident, whereas all parents of Langer syndrome-affected patients display the above-described symptoms of dyschondrosteosis. Neither ankle nor carpo-tarsal coalitions are present in Langer type. Conversely, carpal and tarsal synostoses are recognized in Nievergelt mesomelic dysplasia [12]. Characteristic of this disease, the massive carpo-tarsal coalitions may extend to metacarpals/metatarsals and phalanges. In conjunction with clubfoot deformity, these symptoms to some extent may resemble Kantaputra mesomelia. Bilateral elbow dysplasia, forearm shortening, brachy and clinocamptylodactylia may be subject to incomplete phenotypic expression. The lower leg dysplasia ranges from mere involvement through moderate tibial and fibular dysplasia with exostoses to severely deficient, rudimentary rhomboid tibia accompanied by cutaneous dimples. The ankle synostoses have not been reported. Thus, a very careful radiological assessment should allow for differentiation of these seemingly alike diseases.

Carpo-tarsal synostoses may be inconstant findings for Kantaputra type; however, often they are simply overlooked on plain radiographs because of bone maturation delay and their chondrodesmotic character. Similar reasoning applies to diagnosis of conceivable carpo-tarsal deficiencies. Bone deficiency is accredited to a radiological appearance of delayed ossification, and conversely, at a later age, to multiple bony fusions and misshaping. In our patient neither carpal synostoses nor deficits have been diagnosed, but it cannot be excluded that they will gradually become apparent. Similarly, lower leg synostoses were primary not distinguishable with plain radiography. Magnetic resonance imaging of tarsi revealed fibulo-calcanear and tibio-talar incomplete synostoses additionally fused at talo-calcanear level and accompanied by an accessory bone within the talo-calcanear joint. A complete, bony fusion is evident on radiographs of adult patients with Kantaputra type [1,2]. Magnetic resonance is an effective imaging modality that allows an explanation of the nature of incomplete synostosis encountered in children [14]. Owing to a nonfibrous but cartilaginous character of the coalition, this is a primary formation. It develops intrauterinally, rather as a defect of differentiation of cartilaginous tarsals into separate elements, not as a secondary fusion of already well-delineated units. Lack of fusion lines in ankle coalitions of previously reported adult patients also confirms this hypothesis [1]. Although tarsal synostoses may not appear in all affected patients, fibulo-calcanear fusion is a constant finding in Kantaputra type. Moreover, to the best of our knowledge, there have been no reports in the English literature on congenital ankle synostosis, neither as an idiopathic finding nor as a composite of any syndrome. Thus, primary fibulo-calcaneal synostosis appears to be a pathognomonic sign for Kantaputra type.

An interesting finding in our patient was an accessory calcaneal ossification center. The small posterior nucleus became fused to the main calcaneus at 2 years of age. The calcaneus begins ossification at the end of the second trimester of fetal life. Contrary to the majority of tarsal bones, it is already evident on radiographs at birth. Hardly

Table 2 **Differentiation between mesomelic dysplasias**

Mesomelic dysplasia	Kantaputra [1–5]	Leri–Weil [7]	Langer [8]	Robinow AD/AR [9]	Savarirayan [10]	Kozlowski–Reardon [11]	Nievergelt 12]	Acral synostoses [13]
Symptoms								
OMIM	156232	127300	249700	180700/ 268310	605274	249710	163400	600383
Inheritance	AD	Pseudo-AD	Pseudo-AR	AD/AR	SP	AR	AD	AD
Short stature	Y	N/Y	Y	Y		Y	Y	Y
Craniofacial dysmorphism	N	N	N	Y	Y/N	Y	N	Y
Delayed milestones	N	N	N	N/Y	Y	N	Y/N	Y
Lower intelligence	N	rarely	N	N	Y	N	N	N
Normal karyotype	Y	t X/Y	Y	Y	Y	Y	Y	
Mutation	2q24-q32	Pseudoautos. region Xp22, SHOX		9q22 ROR2			Different expression of the same autosome mutation	
Shortening of forearms	Y	Y	Y	Y		Y	Y/N	
Elbow abnormality	Y	Y	Y			Y	Y	Y
Radial head dislocation	Y	Y			Y	Y	Y	Y
Ulna shorter than radius	Y	Y	Y	Y		N		Y
Ulnar head dislocation		Y		Y		N	Y	
Hand ulnar deviation	Y	Y	Y	Y		N		Y
Carpal synostoses	Y*			Y		N	Y	
Defects of metacarpals or phalanges	Y/N			Y	N	Y	Y/N	Y
Phalangeal joint contractures	Y/N					N	Y/N	
Shortening of lower legs	Y	N/Y	Y	Y		Y		
Deformation/shortening of tibia	Y	Y/N	Y	Y	Y	Y	Y	Y
Deformation/shortening of fibula	Y	Y/N	Y	Y	Y	Y	Y/N	Y
Tiptoe gait	Y		Y			Y		
Pes equinus/equinovarus	Y	N	Y		Y	Y	Y/N	
Tarsal synostoses	Y/N	N				N	Y	
Ankle synostoses	Y/N	N				N		Y
Talus/calcaneus malformation	Y	N				Y		Y
Defects of metatarsals or phalanges	N	N			N		Y	Y
Hip dysplasia	N	N			Y	Y	Y/N	
Cutaneous malformations over limbs	N	N				Y	Y	
Spine deformity				Y		Y		
Extraskeletal involvement	N	N		Y	Y	N	Y	Y
Others		Prevalence in females, muscular hypertrophy in males	Parents affected with Leri–Weill					

Autosom., autosomal; OMIM, online Mendelian inheritance in man; pseudoautos., pseudoautosomal.
*Not all patients.

ever does the ossification center reveal a split [15]. An autonomous existence of bifid calcaneus is extremely rare. More often it has been reported as a component of congenital diseases such as Down syndrome, Larsen syndrome, or mucolipidoses [16]. Coexistence with various inheritable syndromes and a bilateral involvement suggest it is not coincidental in our patient. Although the accessory calcaneal ossification center has not been reported earlier, it may be an integral element of Kantaputra mesomelia.

The nosologic classification of genetic skeletal disorders is undergoing constant fluctuation, with a variety of syndromes overlapping, changing categories, or undergoing group fusions, with some cases not classified yet. The clinical evaluation is demanding. It may be difficult to distinguish and uniformly catalog certain dysplasias. Systematic and careful assessment of clinical symptoms supported by plain radiography, combined with a profound MRI analysis, especially of ankle involvement, allows adequate diagnosis in detecting Kantaputra type – the ankle, carpal, tarsal synostoses mesomelic dysplasia, even at a young age.

References

1 Kantaputra PN, Gorlin RJ, Langer LO. Dominant mesomelic dysplasia, ankle, carpal and tarsal synostosis type: a new autosomal dominant bone disorder. *Am J Med Genet* 1992; **16**:589–594.

2 Shears DJ, Offiah A, Rutland P, Sirimanna T, Bitner-Glindzicz M, Hall C. Kantaputra mesomelic dysplasia: a second reported family. *Am J Med Genet* 2004; **128A**:6–11.

3 Kwee ML, Van de Sluijs JA, van Vugt JM, Gille JJ. Mesomelic dysplasia, Kantaputra type: clinical report, prenatal diagnosis, no evidence for SHOX deletion/mutation. *Am J Med Genet* 2004; **128A**:404–409.

4 Kantaputra PN. Thirteen-year-follow up report on mesomelic dysplasia, Kantaputra type (MDK), and comments on the paper of the second reported family of MDK by Shears et al. *Am J Med Genet* 2004; **128A**:1–5.
5 Fujimoto M, Kantaputra PN, Ikegawa S, Fukushima Y, Sonta S, Matsuo M, *et al*. The gene for mesomelic dysplasia Kantaputra type is mapped to chromosome 2q24-q32. *J Hum Genet* 1998; **43**:32–36.
6 Superti-Furga A, Unger S. Nosology and classification of genetic skeletal disorders: 2006 revision. *Am J Med Genet A* 2007; **143A**:1–18.
7 Mohan V, Gupta RP, Helmi K, Marklund T. Leri-Weill syndrome (dyschondrosteosis): a family study. *J Hand Surg (Br)* 1988; **13**: 16–18.
8 Kunze J, Klemm T. Mesomelic dysplasia, type Langer-A homozygous state for dyschondrosteosis. *Eur J Pediatr* 1980; **134**:269–272.
9 Patton MA, Afzal AR. Robinow syndrome. *J Med Genet* 2002; **39**: 305–310.
10 Savarirayan R, Cormier-Daire V, Curry CJ, Nashelsky MB, Rappaport V, Rimoin DL, Lachman RS. New mesomelic dysplasia with absent fibulae and triangular tibiae. *Am J Med Genet* 2000; **94**:59–63.
11 Reardon W, Hall CM, Slaney S, Huson SM, Connell J, al-Hilaly N, *et al*. Mesomelic limb shortness: a previously unreported autosomal recessive type. *Am J Med Genet* 1993; **47**:788–792.
12 Pearlman HS, Edkin RE, Warren RF. Familial tarsal and carpal synostosis with radial-head subluxation (Nievergelt's Syndrome). *J Bone Joint Surg Am* 1964; **46**:585–592.
13 Leroy JG, Claus L, Lee B, Mortier GR. Mesomelic dysplasia with specific autopodal synostoses: a third observation and further delineation of the multiple congenital anomaly syndrome. *Pediatr Pathol Mol Med* 2003; **22**:23–35.
14 Newman JS, Newberg AH. Congenital tarsal coalition: multimodality evaluation with emphasis on CT and MR imaging. *Radiographics* 2000;**20**:321–332.
15 Tachdjian MO. Introduction. In: Tachdjian MO, editor. *The child's foot*. Philadelphia: W. B. Saunders; 1985: 1–131.
16 Turhan AU, Dinç H, Aydin H, Aynaci O. An accessory ossification centre in the calcaneus with talonavicular and second metatarsocuneiform coalitions. *Eur Radiol* 1999; **9**:481–482.

The effect of the platelet concentration in platelet-rich plasma gel on the regeneration of bone

M. Kawasumi,
H. Kitoh,
K. A. Siwicka,
N. Ishiguro

From Nagoya University School of Medicine, Nagoya, Japan

The aim of our study was to investigate the effect of platelet-rich plasma on the proliferation and differentiation of rat bone-marrow cells and to determine an optimal platelet concentration in plasma for osseous tissue engineering. Rat bone-marrow cells embedded in different concentrations of platelet-rich plasma gel were cultured for six days. Their potential for proliferation and osteogenic differentiation was analysed. Using a rat limb-lengthening model, the cultured rat bone-marrow cells with platelet-rich plasma of variable concentrations were transplanted into the distraction gap and the quality of the regenerate bone was evaluated radiologically.

Cellular proliferation was enhanced in all the platelet-rich plasma groups in a dose-dependent manner. Although no significant differences in the production and mRNA expression of alkaline phosphatase were detected among these groups, mature bone regenerates were more prevalent in the group with the highest concentration of platelets.

Our results indicate that a high platelet concentration in the platelet-rich plasma in combination with osteoblastic cells could accelerate the formation of new bone during limb-lengthening procedures.

There is currently an increased interest in the use of platelet-rich plasma for bone regeneration and healing. It contains osteo-inductive growth factors including platelet-derived growth factors, vascular endothelial growth factor, insulin-like growth factor and transforming growth factors.[1-5] These cause the proliferation and differentiation of local osteoprogenitor cells into bone-forming cells, leading to mineralisation and the formation of bone matrix.[6,7] It has been shown, however, that variations in the concentration of platelets in the platelet-rich plasma have diverse effects on the proliferation and differentiations of the osteoblasts.[8-14] Choi et al[8] reported that the viability and proliferation of alveolar bone cells were suppressed by a high, and stimulated by a low concentration of platelets in the platelet-rich plasma. Uggeri et al[14] found that proteins released from platelet gel stimulated the proliferation of osteoblasts in a dose-dependent manner. In order to provide clear evidence for the clinical use of platelet-rich plasma, it is necessary to determine its direct effect on osteogenic cells at the cellular and molecular level.

Platelet-rich plasma is an autologous preparation and there are therefore no concerns about the transmission of disease or an immunogenic reaction. There have been several clinical trials using a combination of platelet-rich plasma and bone graft or osteoprogenitor cells which have aimed at increasing the rate of osteogenesis and the enhancement of the formation of bone.[4-19]

We have established a new technique of transplantation using culture-expanded bone-marrow cells and platelet-rich plasma in distraction osteogenesis of the long bones and demonstrated a satisfactory clinical outcome by accelerating the formation of new bone.[15-17] To improve our combined bone-marrow cells and platelet-rich plasma cell therapy further, it was necessary to determine the optimal platelet concentration of the plasma for bone regeneration.

Our aim therefore was to evaluate the osteogenic differentiation of rat bone-marrow cells embedded in platelet-rich plasma gels with different platelet concentrations. Using a rat model of limb lengthening, the rat bone-marrow cells and platelet-rich plasma gels were then transplanted into the lengthened femur, and bone formation *in vivo* was analysed.

Materials and Methods

Preparation of platelet-rich plasma gels with different platelet concentrations. Under general anaesthesia whole blood was withdrawn

* M. Kawasumi, MD, Orthopaedic Surgeon
* H. Kitoh, MD, PhD, Orthopaedic Surgeon
* K. A. Siwicka, MD, Orthopaedic Surgeon
* N. Ishiguro, MD, PhD, Professor of Orthopaedics
Department of Orthopaedic Surgery
Nagoya University School of Medicine, 65 Tsurumai-cho, Showa-ku Nagoya, Aichi 466-8550, Japan.

Correspondence should be sent to Dr M. Kawasumi; e-mail: kawasumi@med.nagoya-u.ac.jp

doi:10.1302/0301-620X.90B7.20235 $2.00

J Bone Joint Surg [Br] 2008;90-B:966-72.
Received 24 September 2007; Accepted after revision 7 February 2008

by cardiac puncture from 90 14-week-old male Sprague-Dawley rats (Japan SLC Inc., Shizuoka, Japan). For one series, 40 ml of anticoagulated whole blood was initially centrifuged at 1100 g for ten minutes to precipitate the red blood-cell fraction. The supernatant was again centrifuged to produce precipitation of platelets. The platelet-rich plasma was then divided into three groups (low concentrate; medium; and high concentrate) according to the amount of supernatant which had been removed. We used platelet concentrations as suggested by Marx.[1] The supernatant alone was used as platelet-poor plasma. The number of platelets in the high, medium, low concentrate, platelet-poor plasma and whole blood was counted using a Sysmex XE 2100 haematology analyser (Sysmex, Kobe, Japan).

Bone-marrow cells culture. Specially-prepared minimum essential medium alpha (Gibco-BRL, Carlsbad, California), supplemented with 10% fetal bovine serum (Dainippon Pharmaceutical, Osaka, Japan), 100 µl/ml of penicillin-streptomycin (Gibco-BRL, Life Technologies, Grand Island, New York), 0.2 mM ascorbic acid (Sigma, St Louis, Missouri) 10 mM Na-b-glycerophosphate (Sigma), and 10^{-8}M dexamethasone (Sigma), was used as a growth medium in all the cell-culture experiments.

Rat bone-marrow cells were isolated from 60 four-week-old, male Sprague-Dawley rats weighing between 90 g and 110 g using the technique described by Takamine et al.[20] The harvested cells were cultured with 8 ml of growth medium. The adherent cells were expanded as monolayer cultures in a 5% CO_2/95% air atmosphere at 37°C with medium changes every three days. When the cultures became nearly confluent, the cells were dissociated with 0.25% trypsin/ethylenediaminetetraacetic acid (EDTA) (Gibco BRL) and re-seeded at a density of 3×10^5 cells/dish. Cells passaged twice (P2) were used for all three-dimensional (3-D) cultures.

3-D gel-embedded culture of rat bone-marrow cells. A suspension of 8×10^4 rat bone-marrow cells in 150 µl of each platelet derivative was mixed with 50 µl of a thrombin/$CaCl_2$ solution to obtain platelet gel. The rat bone-marrow cells were also mixed with bovine-dermal-pepsin-solubilised type-I collagen (Koken Co., Ltd, Tokyo, Japan) in gel form at 37°C. The rat bone-marrow cells embedded in gel at a density of 4×10^5 cells/ml were cultured for six days and were then divided into five groups (group P, embedded in the platelet-poor plasma gel; group L, embedded in the low concentration gel; group M, embedded in the medium concentration gel; group H, embedded in the high concentration gel; and group C, embedded in the collagen gel).

***In vitro* cell proliferation.** The WST-1 cell proliferation reagent (Roche Diagnostics GmbH, Mannheim, Germany) was used for counting the cells.[11,21] The WST-1 test measures the mitochondrial activity which corresponds to the number of viable cells. After incubation for one hour at 37°C, the absorption of the medium containing the WST-1 reagent was measured by an enzyme-linked immunoabsorbent assay (ELISA) Reader (Thermo Fisher Scientific Inc., Waltham, Massachsetts) at 440 nm with a reference wavelength > 600 nm. The WST-1 assay was carried out at intervals of two days after the initiation of the 3-D cultures. Each experiment was repeated twice with 20 samples for each group, resulting in a total of 40 samples per group.

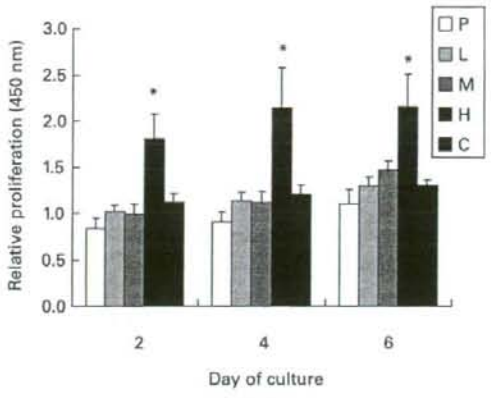

Fig. 1

Graph showing the number of viable rat bone-marrow cells cultured with platelet-rich plasma gels with different concentrations of platelets and collagen gel. Cell proliferation was significantly enhanced in group H. (P, platelet-poor plasma; L, low concentration platelet-rich plasma; M, medium concentration platelet-rich plasma; H, high concentration platelet-rich plasma; C, collagen gel; *, statistically significant, $p < 0.05$).

***In vitro* osteogenic differentiation.** The cultures were washed in phosphate-buffered saline and the cells were lysed using a UP50H ultrasonic processor (Hielscher Ultrasonics GmbH, Teltow, Germany). Using the alkaline phospha-B-test (Wako, Osaka, Japan), the activity of alkaline phosphatase in the cell lysates was measured every two days after embedding of the cells.

After the gels had been dissolved by urokinase (Uronase; Mochida, Tokyo, Japan) and collagenase (Sigma-Aldrich, Tokyo, Japan), the total RNA was isolated every two days using the RNeasy Mini Kit (QIAGEN KK, Tokyo, Japan). For reverse transcription into circular DNA (cDNA) (reverse transcription system; Perkin Elmer, Waltham, Massachusetts), one µg of RNA was used as a template. cDNA was amplified by the polymerase chain reaction with oligonucleotide primers for alkaline phosphatase and glyceraldehyde-3-phosphate dehydrogenase as housekeeping genes.[22] Quantitative real-time was carried out using a Light Cycler 480 Real-Time System (Roche Diagnostics Corporation, Indianapolis, Indiana) and a Light Cycler Fast Start DNA Master SYBR Green I (Roche Diagnostics Corporation).

Rat model of limb lengthening. All the animal experiments were carried out in compliance with the laws and guidelines for the experimental use and care of animals. Application of an external fixation device to the femora of 91 nine-week-old male Sprague-Dawley rats weighing between

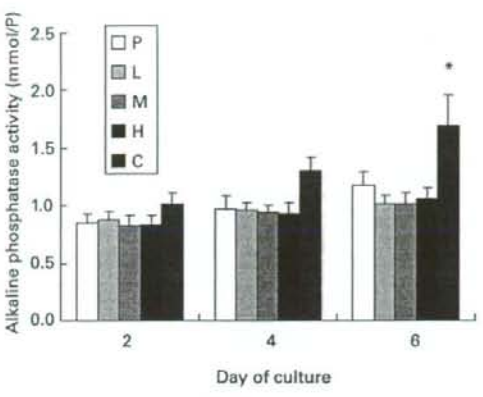

Fig. 2a

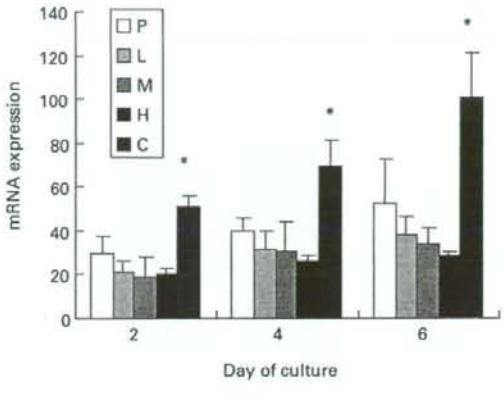

Fig. 2b

Graphs showing a) the concentration of alkaline phosphatase in the cell lysates and b) alkaline-phosphatase expression as measured by mRNA in rat bone-marrow cells cultured with platelet-rich plasma gels of different platelet concentrations and collagen gel. The alkaline phosphatase activity was significantly increased in group C on day six and there was also significantly enhanced expression of alkaline phosphatase mRNA in this group. (P, platelet-poor plasma; L, low concentration platelet-rich plasma; M, medium concentration platelet-rich plasma; H, high concentration platelet-rich plasma; C, collagen gel; *, statistically significant, $p < 0.05$).

320 g and 380 g was followed by an osteotomy at the level of the diaphysis.[20] Weight-bearing as tolerated was allowed immediately after the operation. Seven days after operation lengthening was initiated at a rate of 0.375 mm twice daily for ten days (7.5 cm of total distraction). Immediately after the completion of lengthening, 150 µl of each type of gel containing rat bone-marrow cells at a density of 1×10^7 cells/ml were injected into the distraction callus under fluoroscopic guidance. The rats were divided into five groups, according to the type of injected gel as follows: group P (n = 16), group L (n = 20), group M (n = 20), group H (n = 20), and group C (n = 15).

Radiological evaluation. This was performed using a soft radiograph apparatus (Softex ES/M; Softex Co, Tokyo, Japan). Lateral radiographs were taken at one, two, and four weeks after injection of gel. They were evaluated using image-analysis software (Scion Image for Windows, Scion Co, Frederick, Maryland). The distraction gap was outlined as a quadrilateral region of interest from the outside corners of the two proximal and the two distal cortices. Mineralised new bone was defined as any region with a density equivalent to or greater than the adjacent medullary bone.

***In vivo* micro-CT.** Representative specimens of distracted femora (six rats in each group, 30 in total) were examined using a high-resolution micro-CT imaging system (ScanX-mate-A100S; Comscantecno Co. Ltd, Kanagawa, Japan) four weeks after injection of bone-marrow cells. Volumetric measurements of mineralised new bone were made using 3-D image analysis software (TR1/3D-BON; Ratoc System Engineering Co. Ltd, Tokyo, Japan). The volume of the distraction gap was also recorded and it represented the volume of interest which was mineralised.

Statistical analysis. Equality of variances was verified using the Bartlett test (Stat View for Windows version 5.0; SAS Institute Japan Ltd, Tokyo, Japan). One-way analysis of variance was used for comparison of groups, supported by the Bonferroni-type multiple comparison. Statistical significance was set at a p-value ≤ 0.05. All the results are expressed as the mean and SEM (±).

Results

Properties of platelet-rich plasma and platelet-poor plasma. The mean concentration of platelets (platelets/µl) was $4358 \pm 265 \times 10^3$ in high concentration, $1453 \pm 88 \times 10^3$ in medium concentration, $48 \pm 29 \times 10^3$ in low concentration, $8 \pm 2 \times 10^3$ in platelet-poor plasma and $413 \pm 54 \times 10^3$ in whole blood. The mean concentration of platelets in the low, medium and high concentration groups was 117% (76% to 146%), 352% (263% to 441%) and 1055% (695% to 1233%) of that in whole blood, respectively. There was a ninefold difference in the mean platelet concentration between the low and high concentration groups. There was no significant difference in the concentration of fibrinogen among the groups.

***In vitro* cell proliferation.** Group H showed a significant increase in the proliferation of rat bone-marrow cells compared with the remaining groups on days 2, 4 and 6 (analysis of variance (ANOVA), $p < 0.05$). By contrast, groups L and M did not show increased cell proliferation, compared with group P (Fig. 1).

***In vitro* osteogenic differentiation.** On day 6, the alkaline phosphatase activity was significantly increased in group C (ANOVA, $p < 0.05$), compared with the other groups (Fig. 2a). Group P L, M and H showed no significant increase in

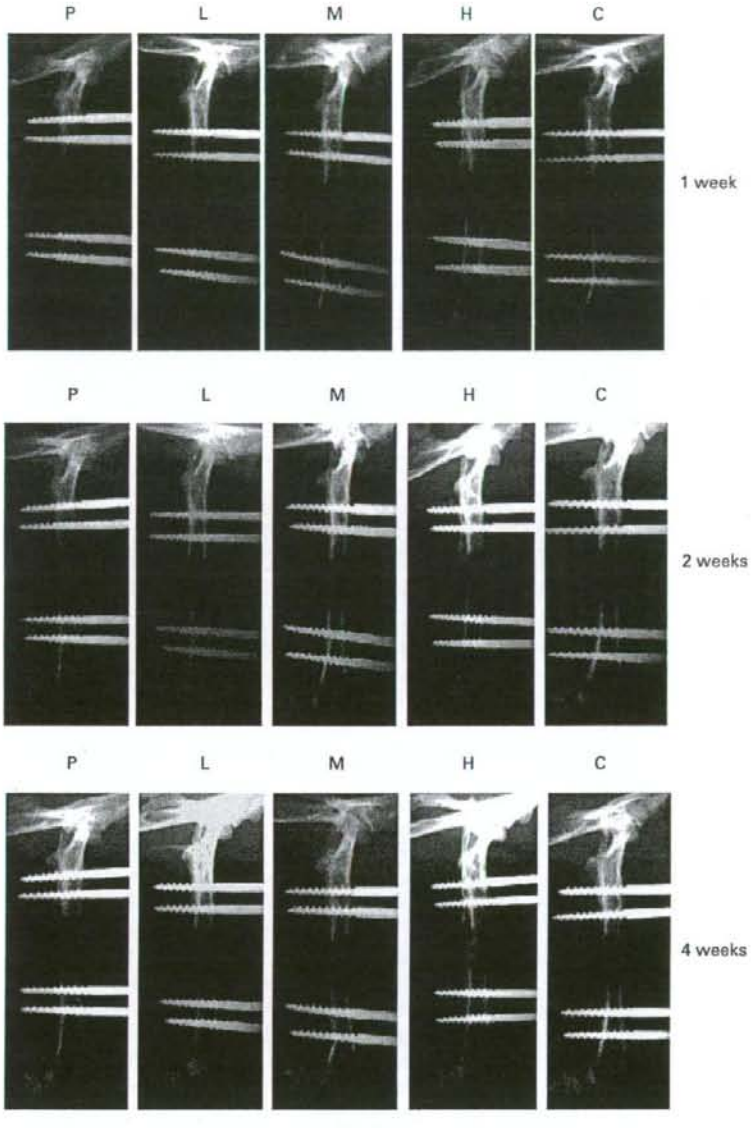

Fig. 3

Plain radiographs of lengthened femora of rats after injection of rat bone-marrow cells embedded in platelet-rich plasma gel with different platelet concentrations or collagen gel into the distraction group. Radiographs were taken at one, two, and four weeks after transplantation. Complete bridging of the gap was observed in group H at four weeks (P, platelet-poor plasma; L, low concentration platelet-rich plasma; M, medium concentration platelet-rich plasma; H, high concentration platelet-rich plasma; C, collagen gel).

alkaline phosphatase activity. Similarly, the expression of alkaline phosphatase mRNA was significantly increased in group C (ANOVA, $p < 0.05$) while there was no significant differences in the other groups (Fig. 2b).

Radiological evaluation. The formation of callus was enhanced in a platelet dose-dependent manner among the scaffolds. At four weeks after completion of distraction, radiological union was evident in group H only. In the

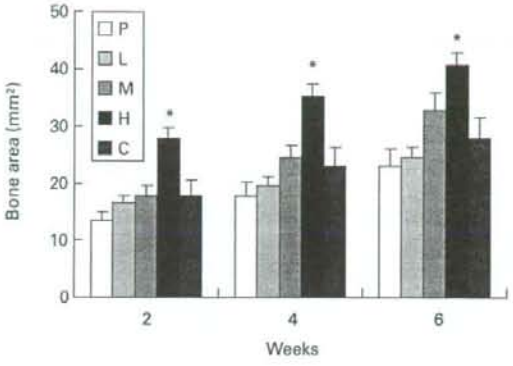

Fig. 4

Graph showing the quantification of mineralised bone area in the distraction callus. Significantly enhanced bone formation was observed in group H (ANOVA, $p < 0.05$) (P, platelet-poor plasma; L, low concentration platelet-rich plasma; M, medium concentration platelet-rich plasma; H, high concentration platelet-rich plasma; C, collagen gel).

remaining groups, the central radiolucent area (fibrous zone) was still present (Fig. 3). In group H, satisfactory formation of callus was seen soon after the injection of the rat bone-marrow cells, resulting in an early bridging of the distraction gap.

Significantly larger areas of mineralised bone were found in group H than in the other groups at four weeks after injection of the rat bone-marrow cells (ANOVA, $p < 0.05$). There were no significant differences in bone formation among groups P, L, M, and C (Fig. 4).

Micro CT. Favourable bone formation was observed in groups H and C (Fig. 5). Quantitative 3-D CT showed that the volume of the distraction gap was largest in group H, although there were no statistically significant differences among any group (Fig. 6).

Discussion

We have previously shown a satisfactory outcome in femoral lengthening enhanced by transplantation of culture-expanded bone-marrow cells and platelet-rich plasma into the callus.[15] However, the beneficial effect of cell therapy on osteogenesis was less pronounced at the anteromedial aspect of the tibia.[16,17] To improve our bone-marrow cells and platet-rich plasma cell therapy, it was necessary to determine the concentration of platelets in the plasma gel which would give the optimal proliferation and differentiation capability of the bone-marrow cells. In our study, the 3-D culture system was used to analyse the proliferation and differentiation of rat bone-marrow cells in platelet-rich plasma gels containing variable concentrations of platelets. In addition, the effect of transplantation of bone-marrow cells on distraction osteogenesis was evaluated *in vivo* in the rat limb-lengthening model. To the best of our knowledge, this is the first report which has investigated the quality of regenerate bone during distraction osteogenesis after transplantation of rat bone-marrow cells combined with variable concentrations of platelets in platelet-rich plasma gel.

Platelet-rich plasma with a higher platelet concentration significantly enhanced the proliferation of rat bone-marrow cells, although the rate of differentiation of osteoblasts was not accelerated. However, the effect of platelet-rich plasma on the proliferation and differentiation of osteoblastic cells is still controversial. Choi et al,[8] using canine platelet-rich plasma and alveolar bone cells, showed that the viability and proliferation of the latter were suppressed by high, but were stimulated by low concentrations of platelet-rich plasma. Kanno et al[23] noted that human platelet-rich plasma inhibited activity in the osteoblastic cell line during the growth phase, but stimulated it when the cells attained confluence. Graziani et al[9] showed that moderate platelet concentrations in human platelet-rich plasma stimulated the differentiation of human osteoblasts. Lucarelli et al[10] stated that 10% platelet-rich plasma promoted the proliferation of stromal stem cells derived from human bone marrow. The results of previous studies may differ from our findings because of the different origins of platelet-rich plasma used or cell types examined. The amount of platelet-rich-plasma-derived growth factors varied depending on the animal species,[24] and the cellular response to these growth factors may also depend on the phenotype of the cells tested. However, similar results were reported by Arpornmaeklong et al[11] and Ogino et al,[12] who analysed the effect of platelet concentrations in rat platelet-rich plasma on the proliferation and differentiation of rat bone-marrow cells. Arpornmaeklong et al[11] noted that platelet-rich plasma caused a dose-dependent stimulation of cell proliferation while reducing alkaline phosphatase activity and calcium deposition in the 3-D culture. Ogino et al[12] showed that platelet-rich plasma stimulated the proliferation but suppressed the differentiation in the monolayer culture system. These studies suggested that platelet-rich plasma could have a beneficial effect on the proliferation of bone-marrow cells, without promoting osteoblastic differentiation.

The quality of the regenerated bone was significantly improved after transplantation of rat bone-marrow cells with a plasma with a higher platelet concentration, although these cells showed no increase in alkaline phosphatase activity in the *in vitro* 3-D culture, compared with gels with a lower concentration of platelets. We have previously observed elevated levels of alkaline phosphatase activity in rat P2 cells cultured with differentiation medium containing dexamethasone.[22] In the present study, the embedded rat P2 bone-marrow cells used for transplantation could have differentiated into an osteoblastic phenotype during the monolayer culture before transplantation into the callus. The positive effect on osteogenesis in group H may have resulted from the increased potential for proliferation of the osteoblastic cells within the gels.

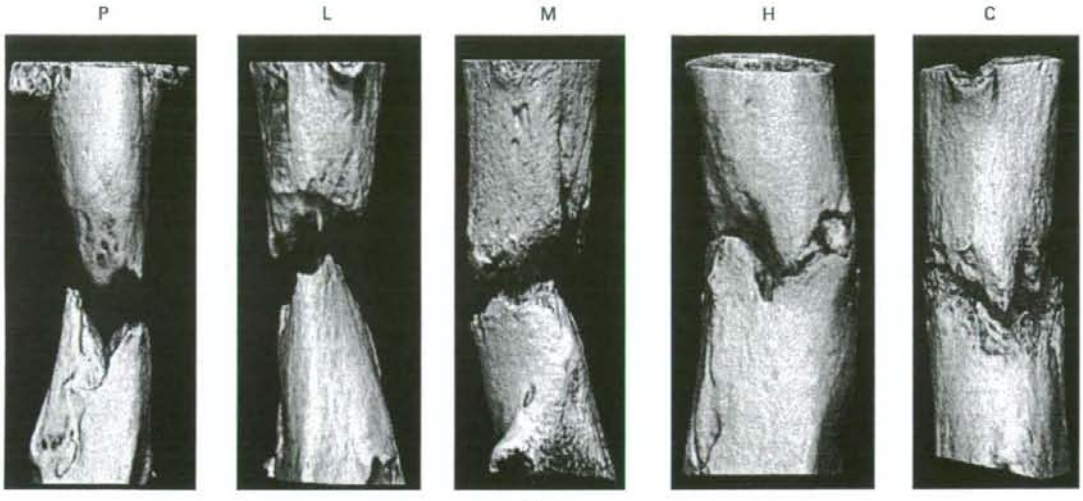

Fig. 5

Micro-CT scans of the distraction gap at four weeks after cell transplantation. Satisfactory bone formation was demonstrated in groups H and C (P, platelet-poor plasma; L, low concentration platelet-rich plasma; M, medium concentration platelet-rich plasma; H, high concentration platelet-rich plasma; C, collagen gel).

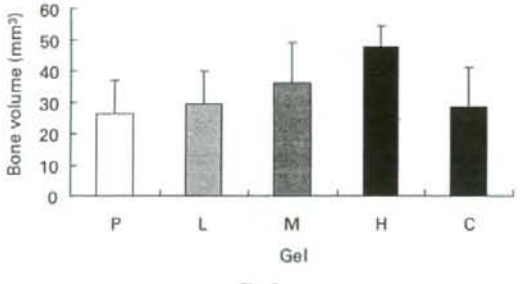

Fig. 6

Graph showing quantitative volumetric analysis of bone regenerates. The largest bone volume was observed in group H (P, platelet-poor plasma; L, low concentration platelet-rich plasma; M, medium concentration platelet-rich plasma; H, high concentration platelet-rich plasma; C, collagen gel).

Rat bone-marrow cells embedded in collagen gels showed the most favourable effect on osteogenic differentiation *in vitro*, and they also resulted in good bone formation *in vivo*. Type-I collagen, as a carrier, is considered to maintain the phenotype of osteoblasts, and the combination of cultured osteoblasts and type-I collagen is commonly-used in tissue engineering.[25,26] We have previously demonstrated that culture-expanded bone-marrow cells mixed with collagen gel accelerated the maturation of regenerate bone and shortened the consolidation period during distraction osteogenesis in rats.[20] Type-I collagen is, however, typically obtained from bovine hides and has the associated risks of immune reaction and disease transmission. On the other hand, autologous platelet-rich plasma is non-toxic and non-immunoreactive and appears to be safe for clinical use. Bone-marrow cells with a high concentration of platelet-rich plasma showed lower alkaline phosphatase activity and mRNA expression compared with those with collagen gels, but transplantation of bone-marrow cells and high concentration platelet-rich plasma significantly improved the radiological appearance of regenerate bone. Quantitative micro-CT showed the largest bone volume within the distraction gap of group H, but the small sample sizes precluded the determination of any statistically significant difference between groups C and H. Therefore, a platelet-rich plasma with a higher concentration of platelet could be a safe substitute for collagen scaffolds for bone-marrow cell therapy in distraction osteogenesis.

In conclusion, a higher concentration of platelets in the platelet-rich plasma gel stimulated the proliferation of rat bone-marrow cells, but did not promote osteoblastic differentiations. Rat bone-marrow cells with a higher concentration of platelets in the platelet-rich plasma had the most favourable effect on osteogenesis in the rat limb-lengthening model. Our results indicate that in clinical practice platelet-rich plasma with a high concentration of platelets may be a useful adjunct for bone regeneration during distraction osteogenesis.

No benefits in any form have been received or will be received from a commercial party related directly or indirectly to the subject of this article.

References

1. **Marx RE.** Platelet-rich plasma: evidence to support its use. *J Oral Maxillofac Surg* 2004;62:489-96.
2. **Weibrich G, Kleis WK, Hafner G, Hitzler WE.** Growth factor levels in platelet-rich plasma and correlations with donor age, sex, and platelet count. *J Craniomaxillofac Surg* 2002;30:97-102.
3. **Harrison P, Cramer EM.** Platelet alpha-granules. *Blood Rev* 1993;7:52-62.
4. **Marx RE, Carlson ER, Eichstaedt RM, et al.** Platelet-rich plasma: growth factor enhancement for bone grafts. *Oral Surg Oral Med Oral Pathol Oral Radiol Endod* 1998;85:638-46.
5. **Schilephake H.** Bone growth factors in maxillofacial skeletal reconstruction. *Int J Oral Maxillofac Surg* 2002;31:469-84.
6. **Fennis JP, Stoelinga PJ, Jansen JA.** Mandibular reconstruction: a clinical and radiographic animal study on the use of autogenous scaffolds and platelet-rich plasma. *Int J Oral Maxillofac Surg* 2002;31:281-6.
7. **Robiony M, Polini F, Costa F, Politi M.** Osteogenesis distraction and platelet-rich plasma for bone restoration of the severely atrophic mandible: preliminary results. *J Oral Maxillofac Surg* 2002;60:630-5.
8. **Choi BH, Zhu SJ, Kim BY, et al.** Effect of platelet-rich plasma (PRP) concentration on the viability and proliferation of alveolar bone cells: an in vitro study. *Int J Oral Maxillofac Surg* 2005;34:420-4.
9. **Graziani F, Ivanovski S, Cei S, et al.** The in vitro effect of different PRP concentrations on osteoblasts and fibroblasts. *Clin Oral Implants Res* 2006;17:212-19.
10. **Lucarelli E, Beccheroni A, Donati D, et al.** Platelet-derived growth factors enhance proliferation of human stromal stem cells. *Biomaterials* 2003;24:3095-100.
11. **Arpornmaeklong P, Kochel M, Depprich R, Kübler NR, Würzler KK.** Influence of platelet-rich plasma (PRP) on osteogenic differentiation of rat bone marrow stromal cells: an in vitro study. *Int J Oral Maxillofac Surg* 2004;33:60-70.
12. **Ogino Y, Ayukawa Y, Tsukiyama Y, Koyano K.** The effect of platelet-rich plasma on the cellular response of rat bone marrow cells in vitro. *Oral Surg Oral Med Oral Pathol Oral Radiol Endod* 2005;100:302-7.
13. **Soffer E, Ouhayound JP, Dosquet C, Meunier A, Anagostou F.** Effects of platelet lysates on select bone cell functions. *Clin Oral Implants Res* 2004;15:581-8.
14. **Uggeri J, Belletti S, Guizzardi S, et al.** Dose-dependent effects of platelet gel releasate on activities of human osteoblasts. *J Periodontol* 2007;10:1985-91.
15. **Kitoh H, Kitakoji T, Tsichiya H, et al.** Transplantation of marrow-derived mesenchymal stem cells and platelet-rich plasma during distraction osteogenesis: a preliminary result of three cases. *Bone* 2004;35:892-8.
16. **Kitoh H, Kitakoji T, Tsuchiya H, Katoh M, Ishiguro N.** Transplantation of culture expanded bone marrow cells and platelet rich plasma in distraction osteogenesis of the long bones. *Bone* 2007;40:522-8.
17. **Kitoh H, Kitakoji T, Tsuchiya H, Katoh M, Ishiguro N.** Distraction osteogenesis of the lower extremity in patients with achondroplasia/hypochondroplasia treated with transplantation of culture-expanded bone marrow cells and platelet-rich plasma. *J Pediatr Orthop* 2007;27:629-34.
18. **Filho Cerruti H, Kerkis I, Kerkis A, et al.** Allogenous bone grafts improved by bone marrow stem cells and platelet growth factors: clinical case reports. *Artif Organs* 2007;31:268-73.
19. **Yamada Y, Ueda M, Hibi H, Baba S.** A novel approach to periodontal tissue regeneration with mesenchymal stem cells and platelet-rich plasma using tissue engineering technology: a clinical case report. *Int J Periodontics Restorative Dent* 2006;26:363-9.
20. **Takamine Y, Tsuchiya H, Kitakoji T, et al.** Distraction osteogenesis enhanced by osteoblast like cells and collagen gel. *Clin Orthop* 2002;399:240-6.
21. **Nasreen N, Mohammed KA, Antony VB.** Silencing the receptor EphA2 suppresses the growth and haptotaxis of malignant mesothelioma cells. *Cancer* 2006;107:2425-35.
22. **Sugiura F, Kitoh H, Ishiguro N.** Osteogenic potential of rat mesenchymal stem cells after several passages. *Biochem Biophys Res Commun* 2004;316:233-9.
23. **Kanno T, Takahashi T, Tsujisawa T, Ariyoshi W, Nishihara T.** Platelet-rich plasma enhances human osteoblast-like cell proliferation and differentiation. *J Oral Maxillofac Surg* 2005;63:362-9.
24. **van den Dolder J, Mooren R, Vloon AP, Stoelinga PJ, Jansen JA.** Platelet-rich plasma: quantification of growth factor levels and the effect on growth and differentiation of rat bone marrow cells. *Tissue Eng* 2006;12:3067-73.
25. **Minamide A, Yoshida M, Kawakami M, et al.** The use of cultured bone marrow cells in type I collagen gel and porouse hydroxyapatite for posterolateral lumbar spine fusion. *Spine* 2005;30:1134-8.
26. **Themistocleous GS, Katopodis HA, Khaldi L, et al.** Implants of type I collagen gel containing MG-63 osteoblast-like cells can act as stable scaffolds stimulating the bone healing process at the sites of the surgically-produced segmental diaphyseal defects in male rabbits. *In Vivo* 2007;21:69-76.

A Histological and Ultrastructural Study of the Iliac Crest Apophysis in Legg-Calve-Perthes Disease

Hiroshi Kitoh, MD, Takahiko Kitakoji, MD, Motoaki Kawasumi, MD, and Naoki Ishiguro, MD

Background: Legg-Calve-Perthes disease (LCPD) is a common hip disorder in children characterized by avascular necrosis of the proximal capital femoral epiphysis. The underlying etiology of the vascular disturbance is still unknown, but it is suggested that LCPD may be a part of a generalized constitutional disorder associated with growth disturbance of bone and cartilage tissue. In this study, the biopsy specimens of the iliac crest apophysis from LCPD patients were examined histologically and ultrastructurally to determine preexisting generalized abnormalities of endochondral ossification.

Methods: Iliac crest apophysis cartilage was taken during Salter innominate osteotomy from 11 children (8 boys and 3 girls) with LCPD at an average age of 7.8 years. As controls, the samples were also obtained from 10 children (2 boys and 8 girls) at an average age of 6.3 years undergoing Salter osteotomy due to residual acetabular dysplasia after reduction of developmental dysplasia of the hip. Each iliac crest apophysis specimen was examined histologically (Toluidine blue staining and Sudan III staining) and ultrastructurally.

Results: Although there were no obvious differences in Toluidine blue–stained sections of the iliac crest cartilage between LCPD and control patients, the Sudan III–positive chondrocytes in the resting cartilage were more prominent in the LCPD specimens than in the control specimens. These sudanophilic granules were confirmed to be lipid droplets by electron microscopic examinations. Ultrastructural examinations of the resting chondrocytes from 3 LCPD patients demonstrated numerous cytoplasmic inclusion bodies with electron dense materials, which were similar to those seen in some of the mucopolysaccharidoses.

Conclusions: Increased lipid droplets and numerous cytoplasmic inclusions filled with fibrillar materials were suggestive of the initial metabolic changes of the chondrocytes, which may have a pivotal role in degenerating matrix and lead to vulnerability of the cartilage tissue. Our results indicated that generalized insufficiency in growth cartilage metabolism may be related to the onset of the disease in some LCPD patients.

Key Words: Legg-Calve-Perthes disease, iliac crest apophysis, ultrastructure, lipid inclusions, chondrocyte metabolism

(*J Pediatr Orthop* 2008;28:435–439)

From the Department of Orthopaedic Surgery, Nagoya University School of Medicine, Nagoya, Aichi, Japan.

This study was conducted at the Department of Orthopaedic Surgery, Nagoya University School of Medicine, Nagoya, Aichi, Japan.

Supported by a Grant-in-Aid for Scientific Research from the Ministry of Education, Culture, Sports, Science and Technology of Japan (contact grant no. 19591755).

None of the authors received financial support for this study.

Reprints: Hiroshi Kitoh, MD, Department of Orthopaedic Surgery, Nagoya University School of Medicine, 65 Tsurumai-Cho, Showa-ku, Nagoya, Aichi 466-8550, Japan. E-mail: hkitoh@med.nagoya-u.ac.jp.

Legg-Calve-Perthes disease (LCPD) is a form of avascular necrosis of the proximal capital femoral epiphysis in children. Various genetic, epidemiological, biochemical, and other factors associated with this condition have been studied, but the etiology remains obscure. Affected children generally have shorter stature than average and delayed skeletal maturation at the onset of the disease.[1,2] The authors demonstrated that ossification of the capital femoral epiphysis is also delayed in LCPD.[3] Guerado and Garces[4] reported that 7 of 16 patients with a previous history of LCPD had some radiological abnormalities of the spine. The authors also showed abnormal sagittal spinal alignment probably due to growth disturbance of the vertebral bodies in patients with LCPD.[5] These clinical and radiological observations have suggested that this disease is a manifestation of a generalized condition associated with growth disturbance of bone and cartilage tissues and abnormalities of proportionate growth in various regions of the body. In this study, the iliac crest growth cartilage of LCPD patients was examined histologically and ultrastructurally to determine preexisting generalized abnormalities of endochondral ossification.

METHODS

After informed consent was obtained from all individuals before the surgery, iliac crest apophysis cartilage was taken during Salter innominate osteotomy from 11 children (8 boys and 3 girls) with LCPD at an average age of 7.8 years (6.2–10.5 years). The diagnosis of LCPD was based on the children's history, results of physical examinations, and radiographs of the hip that showed typical changes within the capital femoral epiphysis and proximal femoral metaphysis. Exclusion criteria included a history of major steroid use, epiphyseal dysplasia, hormonal abnormality, metabolic bone disease, and other known causes of osteonecrosis. As controls, the samples were also obtained, under informed consent, from 10 children (2 boys and 8 girls) at an average age of 6.3 years (5.7–7.5 years) undergoing Salter osteotomy due to residual acetabular dysplasia after reduction of developmental dysplasia of the hip. Each iliac crest apophysis specimen was cut into 3 pieces for histological and ultrastructural examinations.

One of the 3 pieces from each specimen was fixed overnight in 10% neutral-buffered formalin, embedded in paraffin, and cut into sections 6 μm thick. Sections were then stained with Toluidine blue for 30 minutes to estimate the proteoglycan content. The other piece was stored in liquid nitrogen until sectioned and stained. Before sectioning, the samples that had been placed in 10% neutral-buffered formalin were quenched so that they can be sectioned in a cryostat microtome. Serial 10-μm frozen sections were cut from each sample with a cryostat microtome. The slices were washed

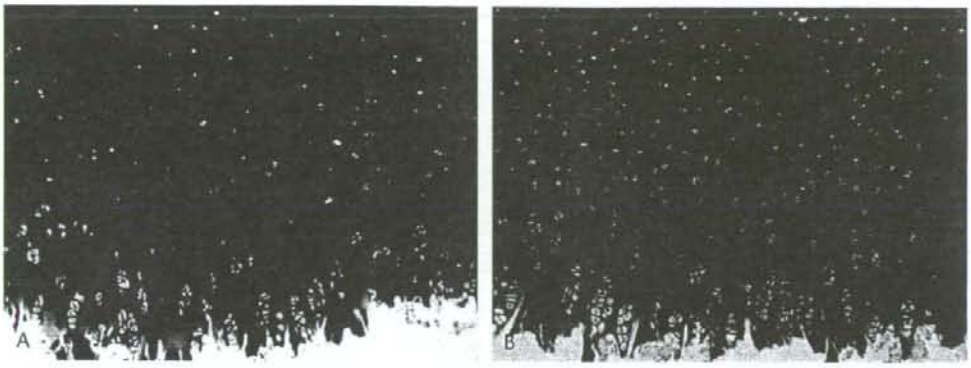

FIGURE 1. Histological sections of the iliac crest growth cartilage from patients L-8 (A) and C-4 (B) demonstrating normal morphological appearance (Toluidine stained; original magnification ×100).

with phosphate-buffered saline and washed briefly with 50% alcohol to give them high affinity for the Sudan III solution. They were then stained in Sudan III for 60 minutes at 37°C and counterstained for 5 minutes with Mayer hematoxylin. Finally, they were rinsed with phosphate-buffered saline for 10 minutes, washed with distilled water, and mounted with glycerol gelatin.

For electron microscopy, the remaining small specimen was fixed in 2% glutaraldehyde in 0.1 mol sodium cacodylate buffer for 3 hours at ice bath and rinsed thoroughly in 0.1 mol cacodylate buffer overnight. The specimens were then postfixed in 2% osmium tetroxide for 3 hours and rapidly dehydrated in increasing concentrations of ethanol from 70% to 100%, cleared in propylene oxide, and embedded in epon. Once appropriate regions for ultrastructural assessment were identified, the blocks were trimmed, sectioned at 70 to 80 nm, stained with lead citrate and uranyl acetate, and examined on a JEOL JEM-2000EX (JEOL Ltd, Japan) transmission electron microscope.

RESULTS

Toluidine Blue Staining

The iliac crest apophysis has clearly delineated histological appearance involving a resting and a growth cartilage layer. The resting cartilage was characteristic of cartilage elsewhere with ovoid chondrocytes and a clear, evenly staining matrix. The chondro-osseous junction showed chondrocyte clusters with normal hypertrophic cell morphology and well-organized column formation. Histological sections from LCPD patients were of normal appearance, and there were no obvious differences in Toluidine blue-stained sections of the iliac crest cartilage between LCPD and control patients (Fig. 1A, B).

Sudan III Staining

We performed a staining with Sudan III to examine the lipid accumulation. This dye is specific for the detection of neutral lipids and fatty acids. Although the Sudan III–positive granules of variable number and size were present in the chondrocytes throughout the depth of the specimens, the inclusions of the chondrocytes were prominent in the chondro-osseous junction compared with the resting cartilage in both groups. No obvious difference in sudanophilia was demonstrated in the chondro-osseous region of the specimens between LCPD and control patients. In the resting cartilage, however, the number of the Sudan III–positive chondrocytes was diverse within the specimens. The individual specimens were then classified into 3 groups according to the percentage of the sudanophilic chondrocytes in the resting cartilage (abundant, Sudan III–positive cells exceeded 50% of the

TABLE 1. Histological and Ultrastructural Findings of the Iliac Crest Apophysis from 11 LCPD Patients and 10 Controls

	Sex	Age, y	Sudan III Staining	Enlarged Vacuoles
LCPD patients				
L-1	Male	6.2	Slight	+
L-2	Female	6.6	Moderate	−
L-3	Male	6.7	Slight	−
L-4	Male	7.1	Slight	−
L-5	Female	7.3	Slight	−
L-6	Male	7.4	Abundant	−
L-7	Male	8.3	Slight	−
L-8	Male	8.4	Moderate	−
L-9	Male	8.6	Moderate	+
L-10	Female	8.8	Abundant	−
L-11	Male	10.5	Moderate	+
Control patients				
C-1	Female	5.7	Slight	−
C-2	Female	5.8	Slight	−
C-3	Female	5.8	Slight	−
C-4	Male	5.9	Slight	−
C-5	Female	5.9	Slight	−
C-6	Female	6.2	Slight	−
C-7	Female	6.4	Moderate	−
C-8	Female	6.8	Slight	−
C-9	Female	7	Slight	−
C-10	Male	7.5	Slight	−

chondrocytes in a plane of section; moderate, sudanophilic chondrocytes in 10%–50%; slight, sudanophilic chondrocytes less than 10%). The LCPD specimens (abundant, 2; moderate, 4; slight, 5) demonstrated relative sudanophilia compared with the control specimens (moderate, 1; slight, 9; Table 1). Numerous Sudan III–positive granules were especially observed throughout the resting chondrocytes in the LCPD specimens from a 7.4-year-old boy (L-6) and an 8.8-year-old girl (L-10; Fig. 2).

Transmission Electron Microscopy

Ultrastructural studies confirmed that some chondrocytes in the resting cartilage had round or oval bodies with high electron density within the cytoplasm, suggesting lipid droplets (Fig. 3). In some chondrocytes, the bodies were very large and numerous. The pericellular matrix of the chondrocytes with these lipid droplets, however, was similar to that adjacent to chondrocytes free of morphological lesions. It seemed that collagen fibrils and proteoglycan components were normal in both specimens from LCPD and controls, although no detailed evaluation of these extracellular matrix structures was included in this study. Some of the chondrocytes from 3 LCPD patients (L-1, L-9, and L-11) contained characteristic numerous and enlarged vacuoles within the cytoplasm. Vacuoles occupied most of the cross-sectional area of the cell and contained electron-dense fine fibrillar materials (Fig. 4A). Cell organelles and a nucleus of these cells with numerous vacuoles were disorganized, suggesting ultrastructural evidence of cell death (Fig. 4B).

DISCUSSION

We examined the iliac crest apophysis growth cartilage, which can be easy in biopsy during Salter innominate osteotomy for LCPD containment therapy and for developmental dysplasia of the hip acetabuloplasty, to determine preexisting generalized abnormalities of cartilage metabolism. By histochemical staining and ultrastructural examinations of the chondrocytes of the iliac crest cartilage, the present study illustrated an increase in the localization of intracellular lipids and characteristic vacuolated inclusions in LCPD chondrocytes. To our knowledge, this is the first report delineating morphological abnormalities of the chondrocytes of the iliac crest cartilage in LCPD.

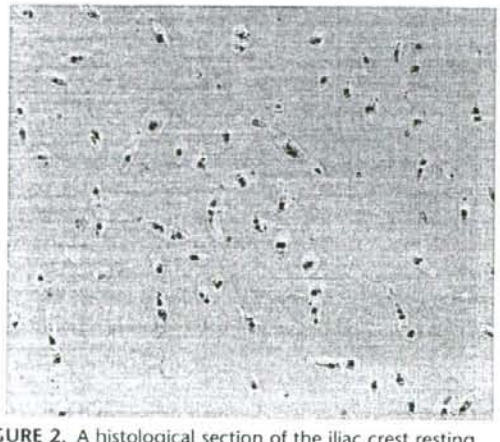

FIGURE 2. A histological section of the iliac crest resting cartilage from patient L-6 showing numerous Sudan III–positive chondrocytes (Sudan III stained; original magnification ×200).

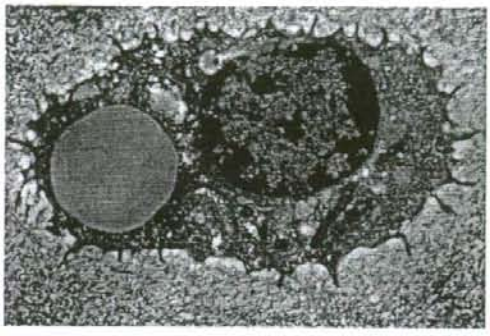

FIGURE 3. A transmission electron micrograph of the iliac crest chondrocyte from patient L-6 demonstrating large round and oval body with high electron density, suggestive of a lipid droplet within the cytoplasm (original magnification ×5000).

Although intracellular lipids have been reported as a constant inclusion in the chondrocytes of hyaline cartilage, lipid accumulation has been observed to be one of the most frequent changes found in degenerating chondrocytes.[6,7] Stanescu et al[8] have described a possible hereditary disorder that produces an accumulation of complex lipids in articular chondrocytes along with precocious arthrosis. Bonner et al[9] showed a progressive intracellular lipid accumulation with age in articular chondrocytes and suggested a possible role for lipid in the initiation of chondrocyte degeneration. Excessive lipid within viable chondrocytes represented the most consistent cellular evidence of proximity to an area of chondronecrosis. Although the biologic significance of lipids in chondrocytes is unknown, it has been postulated that lipids may play a certain role in the metabolism of chondrocytes. Kincaid et al[10] examined the shoulder joint of dogs with osteochondritis dissecans and reported that the lipid inclusions were prominent in pathologic samples. The increase in magnitude of lipids in the pathological cartilage was considered to result from a metabolic response of the chondrocytes to an altered microenvironment. Carlson et al[11] hypothesized that intracellular lipid accumulation resulted from hypoxia/anoxia and may precede matrix degeneration, which precedes cell death. Increased intracellular lipid accumulation may play an important role in the pathogenesis of LCPD, although additional research is needed to determine the role of lipids in the function, metabolism, and homeostasis of cartilage.

It has been suggested that thrombophilia and hypofibrinolysis may be the cause of osteonecrosis. Several investigators have reported that inherited thrombophilic disorders such as deficiencies of protein C, protein S, and mutations of factor V Leiden may be one of the etiologic factors in some cases of LCPD.[12–15] Balasa et al[16] reported that not only the factor V

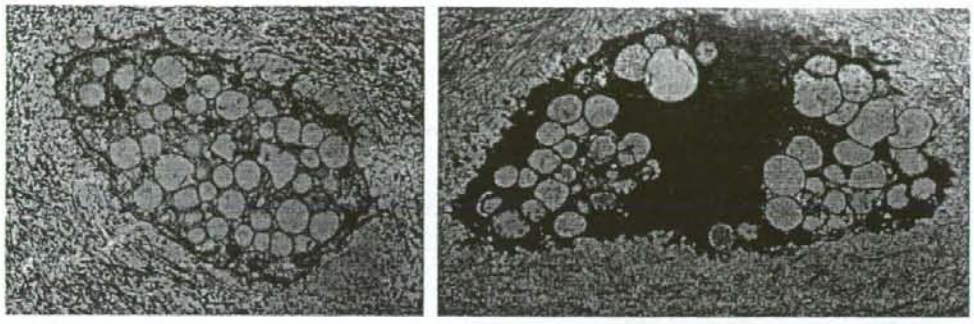

FIGURE 4. Transmission electron micrographs of the iliac crest chondrocyte from patients L11 (A) and L-9 (B) showing numerous enlarged inclusion bodies filled with fine fibrillar materials within the cytoplasm. Cell organelles and a nucleus of these cells were severely disorganized, suggestive of chondronecrosis (original magnification ×5000).

Leiden mutation but also acquired anticardiolipin antibodies, which are believed to cause the thrombosis by inhibiting the action of activated protein C, were associated with the occurrence of LCPD. Abnormalities of protein C, protein S, and factor V Leiden may result in hyperlipidemia, which has been linked to hypercoagulable states and leads to a tendency to thrombosis.[17] Anticardiolipin antibodies may influence lipid metabolism and blood coagulation pathways. These data supported the hypothesis that hypercoagulability and abnormalities of lipid metabolism can contribute to avascular necrosis, although the precise mechanism remains obscure. Increased lipid accumulation in the LCPD chondrocytes suggested an association between the lipid metabolism and the pathogenesis of LCPD. However, we have not examined inherited (protein C, protein S, and factor V Leiden) or acquired (anticardiolipin antibodies) thrombophilic states for the patients with lipid inclusions. Further studies are needed to determine an association between coagulation and lipid disturbances and LCPD.

The vacuolated cells observed in 3 LCPD patients demonstrated characteristic morphology. Ultrastructurally, the content of the enlarged inclusions was mostly fine fibrillar material, and these cells are extremely similar to those observed in some of the mucopolysaccharidoses (MPSs). In MPSs, the appearance of these vacuoles is consistent with that of altered lysosomes. Mucopolysaccharidoses are caused by deficient activity of lysosomal hydrolases that participate in the degradation of glycosaminoglycans; thus, various cell types, including dermal fibroblasts, are affected.[18,19] To examine the existence of systemic diseases such as MPSs, a skin biopsy was performed, under informed consent, from 2 LCPD patients (L-1 and L-9) with numerous cytoplasmic inclusions within chondrocytes during the second surgery for removal of the pins. Transmission electron microscopic examinations of the skin fibroblasts demonstrated that the cell organelles were well organized, and morphological appearance was normal without vacuolated inclusions (Fig. 5).

Legg-Calve-Perthes disease–like hip changes are commonly observed in a few hereditary skeletal dysplasias such as multiple epiphyseal dysplasia (MED) and trichorhinophalangeal syndrome.[20,21] Intracellular inclusions in the chondrocytes have been observed in several chondrodysplasias. Nishimura et al[22] reported cases of spondyloepiphyseal dysplasia with accumulation of periodic acid–Schiff stain–positive inclusion bodies in the chondrocytes. Enlarged rough endoplasmic reticulum inclusion bodies were commonly seen in several skeletal dysplasias, including pseudoachondroplasia, *FGFR3* disorders, and type II collagenopathies.[23–25] The aberrant inclusions due to intracellular retention of mutant molecules may play an important role for pathogenesis of these disorders. In the present study, cytoplasmic inclusion bodies within the chondrocytes of the iliac crest cartilage were observed in some LCPD patients, although accumulated substances have not been fully identified. Legg-Calve-Perthes disease has not been considered to be a skeletal dysplasia, but mild form of some skeletal dysplasias shows minimal skeletal changes indistinguishable to common diseases. The authors previously demonstrated a *COL9A1* mutation in a family with MED.[26] The patients were of normal height with minimal complaints, and the phenotypes of the patients were milder than those of typical MED patients, which were indistinguishable to common idiopathic osteoarthritis. Recently, the authors demonstrated a recurrent mutation in *COL2A1* gene in a

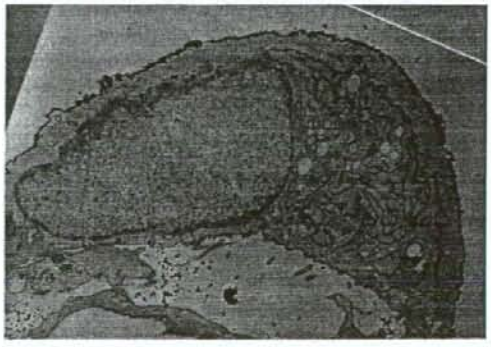

FIGURE 5. A transmission electron micrograph of the skin fibroblast from patient L-9 demonstrating a normal nucleus and cell organelles without vacuolated inclusions (original magnification ×3000).

Japanese family with LCPD.[27] Despite harboring the *COL2A1* mutation, affected family members showed normal stature and minimal radiographic abnormalities except the hip joint. Morphological abnormalities of the iliac crest chondrocytes suggested generalized constitutional disturbance of osteochondrogenesis in LCPD.

There are some limitations in this study. First, a statistical analysis of the differences in sudanophilia between LCPD and control patients has not been performed due to small sample size, and studies on lipid functions and metabolism in patients with increased lipid accumulation have not been carried out. Therefore, it could not be determined if these histological changes are etiologic in LCPD. Second, the possibility of lysosomal changes was speculated in 3 LCPD patients with vacuolated inclusions, but additional stains specific for lysosomes have not been attempted for further investigations.

Several studies have suggested that the vulnerable capital femoral epiphysis can be related to the collapse and necrosis of the femoral head.[3,28] Chondrocytes with increased intracellular inclusion bodies were suggestive of the initial metabolic changes, which may have a pivotal role in degenerating matrix and lead to vulnerability of the cartilage tissue. The vulnerability of the capital femoral epiphysis due to impairment of chondrocyte metabolism may be related to the onset of LCPD in some patients.

REFERENCES

1. Cannon SR, Pozo JL, Catterall A. Elevated growth velocity in children with Perthes' disease. *J Pediatr Orthop*. 1989;9:285–292.
2. Wynne-Davies R, Gormley J. The aetiology of Perthes disease. Genetic, epidemiological, and growth factors in 310 Edinburgh and Glasgow patients. *J Bone Joint Surg Br*. 1978;60:6–14.
3. Kitoh H, Kitakoji T, Katoh M, et al. Delayed ossification of the proximal capital femoral epiphysis in Legg-Calve-Perthes disease. *J Bone Joint Surg Br*. 2003;85:121–124.
4. Guerado E, Garces G. Perthes' disease. A study of constitutional aspects in adulthood. *J Bone Joint Surg Br*. 2001;83:569–571.
5. Kitoh H, Kitakoji T, Katoh M, et al. Sagittal spinal alignment in patients with Legg-Calve-Perthes disease. *Pediatr Int*. 2007;49:612–617.
6. Le Lous M, Corvol MT, Maroteaux P. Lipid composition of two types of chondrocytes in primary culture. *Calcif Tissue Int*. 1981;33:403–407.
7. Lippiello L, Walsh T, Fienhold M. The association of lipid abnormalities with tissue pathology in human osteoarthritic articular cartilage. *Metabolism*. 1991;40:571–576.
8. Stanescu R, Stanescu V, Maroteaux P, et al. Constitutional articular cartilage dysplasia with accumulation of complex lipids in chondrocytes and precocious arthrosis. *Arthritis Rheum*. 1981;24:965–968.
9. Bonner WM, Jonsson H, Malanos C, et al. Changes in the lipids of human articular cartilage with age. *Arthritis Rheum*. 1975;18:461–473.
10. Kincaid SA, Rudd RG, Evander SA. Lipids of normal and osteochondritic cartilage of the immature canine humeral head. *Am J Vet Res*. 1985;46:1060–1065.
11. Carlson CS, Hilley HD, Henrikson CK, et al. The ultrastructure of osteochondrosis of the articular-epiphyseal cartilage complex in growing swine. *Calcif Tissue Int*. 1986;38:44–51.
12. Glueck CJ, Brandt G, Gruppo R, et al. Resistance to activated protein C and Legg-Perthes disease. *Clin Orthop*. 1997;338:139–152.
13. Gruppo R, Glueck CJ, Wall E, et al. Legg-Perthes disease in three siblings, two heterozygous and one homozygous for the factor V Leiden mutation. *J Pediatr*. 1998;132:885–888.
14. Arruda VR, Belangero WD, Ozelo MC, et al. Inherited risk factors for thrombophilia among children with Legg-Calve-Perthes disease. *J Pediatr Orthop*. 1999;19:84–87.
15. Eldridge J, Dilley A, Austin H, et al. The role of protein C, protein S, and resistance to activated protein C in Legg-Calve-Perthes disease. *Pediatrics*. 2001;107:1329–1334.
16. Balasa VV, Gruppo RA, Glueck CJ, et al. Legg-Calve-Perthes disease and thrombophilia. *J Bone Joint Surg Am*. 2004;86:2642–2647.
17. Simpson HC, Mann JI, Meade TW, et al. Hypertriglyceridaemia and hypercoagulability. *Lancet*. 1983;9:786–790.
18. Alroy J, Jones MZ, Rutledge JC, et al. The ultrastructure of skin from a patient with mucopolysaccharidosis IIID. *Acta Neuropathol*. 1997;93:210–213.
19. Nogami H, Oohira A, Suzuki F, et al. Cartilage of I cell disease. *Pediatr Res*. 1981;15:330–334.
20. Dunbar JD, Sussman MD, Aiona MD. Hip pathology in the trichorhinophalangeal syndrome. *J Pediatr Orthop*. 1995;15:381–385.
21. Hesse B, Kohler G. Does it always have to be Perthes' disease? What is epiphyseal dysplasia? *Clin Orthop*. 2003;414:219–227.
22. Nishimura G, Saitoh Y, Okuzumi S, et al. Spondyloepiphyseal dysplasia with accumulation of glycoprotein in the chondrocytes: spondyloepiphyseal dysplasia, Stanescu type. *Skeletal Radiol*. 1998;27:188–194.
23. Vranka J, Mokashi A, Keene DR, et al. Selective intracellular retention of extracellular matrix proteins and chaperones associated with pesudoachondroplasia. *Matrix Biol*. 2001;20:439–450.
24. Brodie SG, Kitoh H, Lachman RS, et al. Platyspondylic lethal skeletal dysplasia, San Diego type, is caused by FGFR3 mutations. *Am J Med Genet*. 1999;84:476–480.
25. Mortier GR, Wilkin DJ, Wilcox WR, et al. A radiographic, morphologic, biochemical and molecular analysis of a case of achondrogenesis type II resulting from substitution for a glycine residue (Gly691→Arg) in the type II collagen trimer. *Hum Mol Genet*. 1995;4:285–288.
26. Nakashima E, Kitoh H, Maeda K, et al. Novel COL9A1 mutation in a family with multiple epiphyseal dysplasia. *Am J Med Genet*. 2005;15:181–184.
27. Miyamoto Y, Matsuda T, Kitoh H, et al. A recurrent mutation in type II collagen gene causes Legg-Calve-Perthes disease in a Japanese family. *Hum Genet*. 2007;121:625–629.
28. Kikkawa M, Imai S, Hukuda S. Altered postnatal expression of insulin-like growth factor–I (IGF-1) and type X collagen preceding the Perthes' disease–like lesion of a rat model. *J Bone Miner Res*. 2000;15:111–119.

ARTHRITIS & RHEUMATISM
Vol. 58, No. 1, January 2008, pp 154–163
DOI 10.1002/art.23175

Regional Differences in Chondrocyte Metabolism in Osteoarthritis

A Detailed Analysis by Laser Capture Microdissection

Naoshi Fukui,[1] Yasuko Ikeda,[1] Toshiyuki Ohnuki,[1] Nobuho Tanaka,[1] Atsuhiko Hikita,[1] Hiroyuki Mitomi,[1] Toshihito Mori,[1] Takuo Juji,[1] Yozo Katsuragawa,[2] Seizo Yamamoto,[3] Motoji Sawabe,[3] Shoji Yamane,[1] Ryuji Suzuki,[1] Linda J. Sandell,[4] and Takahiro Ochi[1]

Objective. **To determine the change in metabolic activity of chondrocytes in osteoarthritic (OA) cartilage, considering regional difference and degree of cartilage degeneration.**

Methods. **OA cartilage was obtained from knee joints with end-stage OA, at both macroscopically intact areas and areas with various degrees of cartilage degeneration. Control cartilage was obtained from age-matched donors. Using laser capture microdissection, cartilage samples were separated into superficial, middle, and deep zones, and gene expression was compared quantitatively in the respective zones between OA and control cartilage.**

Results. **In OA cartilage, gene expression changed markedly with the site. The expression of cartilage matrix genes was highly enhanced in macroscopically intact areas, but the enhancement was less obvious in the degenerated areas, especially in the upper regions. In contrast, in those regions, the expression of type III collagen and fibronectin was most enhanced, suggesting that chondrocytes underwent a phenotypic change there. Within OA cartilage, the expression of cartilage matrix genes was significantly correlated with *SOX9* expression, but not with *SOX5* or *SOX6* expression. In OA cartilage, the strongest correlation was observed between the expression of type III collagen and fibronectin, suggesting the presence of a certain link(s) between their expression.**

Conclusion. **The results of this study revealed a comprehensive view of the metabolic change of the chondrocytes in OA cartilage. The change of gene expression profile was most obvious in the upper region of the degenerated cartilage. The altered gene expression at that region may be responsible for the loss of cartilage matrix associated with OA.**

Osteoarthritis (OA) is a disease characterized by a progressive loss of cartilage matrix that often extends over a decade. During the long course of the disease, chondrocytes undergo obvious metabolic changes. A variety of changes are known to occur that have 2 distinctive aspects. First, the anabolic activity of chondrocytes is strongly enhanced in OA. Following the initial reports more than 4 decades ago (1), an increasing number of studies have shown that the expression of virtually all cartilage components is up-regulated in OA cartilage (2–13). The increased anabolism may be a repair response of the chondrocytes that counteracts the loss of cartilage matrix (2–4). Second, in OA, chondrocytes undergo phenotypic changes. Because of this,

Dr. Fukui's work was supported by Grants-in-Aid from the Japan Society for the Promotion of Science (grants 15390467 and 18390424), the Ministry of Health, Labor, and Welfare of Japan (grant 200500734A), and the Uehara Memorial Foundation, Tokyo, Japan.

[1]Naoshi Fukui, MD, PhD, Yasuko Ikeda, DVM, Toshiyuki Ohnuki, Nobuho Tanaka, BS, Atsuhiko Hikita, MD, PhD, Hiroyuki Mitomi, MD, PhD, Toshihito Mori, MD, Takuo Juji, MD, Shoji Yamane, PhD, Ryuji Suzuki, DVM, PhD, Takahiro Ochi, MD, PhD: National Hospital Organization Sagamihara Hospital, Sagamihara, Japan; [2]Yozo Katsuragawa, MD: International Medical Center of Japan, Tokyo, Japan; [3]Seizo Yamamoto, MD, PhD, Motoji Sawabe, MD, PhD: Tokyo Metropolitan Geriatric Hospital, Tokyo, Japan; [4]Linda J. Sandell, PhD: Washington University School of Medicine, St. Louis, Missouri.

Dr. Sandell has received honoraria (less than $10,000) from GlaxoSmithKline.

Address correspondence and reprint requests to Naoshi Fukui, MD, PhD, Clinical Research Center, National Hospital Organization Sagamihara Hospital, Sakuradai 18-1, Sagamihara, Kanagawa 228-8522, Japan. E-mail: n-fukui@sagamihara-hosp.gr.jp.

Submitted for publication May 22, 2007; accepted in revised form September 14, 2007.

chondrocytes in OA cartilage express matrix genes that are not expressed in normal cartilage, such as type I and type III collagens (5–10). Since the induction of these genes also occurs during the dedifferentiation of chondrocytes in vitro, the phenotypic changes in OA have an aspect resembling that of the dedifferentiation process (9). The phenotypic changes also show a characteristic of developmental reversal, since the expression of type IIA procollagen, a prechondrogenic splicing variant of the type II collagen gene, is observed in OA (11,12). In contrast, the presence of type X collagen in OA cartilage has persuaded investigators that chondrocytes are undergoing hypertrophic changes there (13,14).

Because of the diversity in gene expression, it is currently difficult to obtain a comprehensive idea of the metabolic changes in OA. This diversity may stem from a topographic variation of the pathology. Since cartilage pathology differs obviously from site to site within OA cartilage, it is likely that the metabolic changes in the chondrocytes also differ by areas related to that pathology (4,9,10,15). The regional differences of chondrocyte metabolism may be important to our understanding of the mechanism of disease progression. For example, a focal decline of the matrix synthesis in OA cartilage may play a critical role in the loss of cartilage matrix (3,4,9).

Conventionally, the regional differences of cellular metabolism in OA have been evaluated primarily by histologic methods, so the comparison among the areas has not been quantitative. Laser capture microdissection (LCM) is an innovative technology that enables the isolation of a specific area of tissue by its histologic features (16). Coupled with real-time polymerase chain reaction (PCR), the use of LCM allowed us to perform a quantitative evaluation of the multiple genes expressed in specific regions of OA cartilage. Thus, this study has revealed, for the first time, a comprehensive view of the changes in metabolic activity of chondrocytes in OA cartilage.

MATERIALS AND METHODS

Tissue procurement. This study was performed with the approval of the Human Ethics Review Committees of the participating institutions. For material collection, informed consent was obtained in writing from each subject or family of the donor. OA cartilage samples were obtained from 32 end-stage OA knee joints of 30 patients (mean age 70.3 years [range 56–88 years]) within 4 hours after surgery. The diagnosis of OA was based on the criteria for knee OA of the American College of Rheumatology (17). Control cartilage samples were obtained from 18 nonarthritic knee joints from 16 donors (mean age 82.3 years [range 67–89 years]) within 24 hours after death. The donors had no known history of joint disease or serious trauma, and the normality of the joint was confirmed macroscopically at the time samples were obtained. Knee cartilage in aged donors usually undergoes some degeneration, even though the donors did not have any problems with the joints. Therefore, we obtained control cartilage samples from the knees even when the cartilage showed some signs of degeneration, as long as the degeneration was superficial and limited to small areas (<20% of total cartilage area). Control ligaments, bone tissues, and menisci were also harvested from these joints.

Laser capture microdissection. In each OA joint, cartilage tissues were harvested from 2–5 sites in femoral condyles showing various degrees of cartilage degeneration. In each control joint, cartilage samples were harvested from 2–4 sites in the weight-bearing areas of the femoral condyles. The cartilage samples were cut above the calcified zone, which was confirmed under a microscope at the time of laser microdissection. Immediately after harvest, the cartilage samples were embedded in OCT compound (Sakura Finetechnical, Tokyo, Japan), snap-frozen in liquid nitrogen, and then stored at −80°C until used.

In preparation for LCM, 20–40-μm–thick frozen sections were cut from the cartilage tissues along a plane vertical to the joint surface. The sections were first treated with 0.5*M* EDTA (pH 8.0) for 3 minutes, dehydrated with graded concentrations of ethanol, and clarified with xylene. All reagents were prepared RNase-free, and the entire process was completed within 30 minutes to minimize RNA degradation.

Under an LCM device (PixCell IIe; Arcturus, Mountain View, CA), each frozen section was divided into cartilage zones based on its histologic features (18,19). Cartilage samples from preserved areas contained 3 zones (superficial, middle, and deep) and were separated into these respective zones. For the cartilage from degenerated areas, the number of zones in the section differed from 3 to 1, depending on the severity of the cartilage pathology. A section containing all 3 zones was separated into the 3 respective zones. When a superficial zone was lost to the disease, the section was divided into 2 zones, the middle and deep zones (Figure 1). If a section contained only a deep zone, it was used directly for RNA extraction without microdissection. At each tissue procurement, the appropriateness of zone isolation was confirmed under a microscope.

Analysis of gene expression. Immediately after LCM, RNA was extracted from the tissues using an RNeasy Micro kit (Qiagen, Hilden, Germany) with routine use of DNase I (Qiagen). Complementary DNA (cDNA) was synthesized using Sensiscript reverse transcriptase (Qiagen). Gene expression was evaluated quantitatively by real-time PCR on a LightCycler (Roche Diagnostics, Basel, Switzerland). Gene-specific primers and probes were prepared (a list of primer and probe sequences is available at http://www.hosp.go.jp/~sagami/rinken/crc/index.html), and the process of PCR was monitored by either SYBR Green or hybridization probes. LightCycler FastStart DNA Master SYBR Green I (Roche Diagnostics) or LightCycler FastStart DNA Master Hybridization Probe (Roche Diagnostics) was used for PCR. The PCR protocol was as follows: 95°C for 10 minutes to activate *Taq* polymerase, then 40 cycles of 95°C for 10 seconds, melting temperature for the individual gene for 15 seconds (a list of melting temperatures for the individual genes is available at

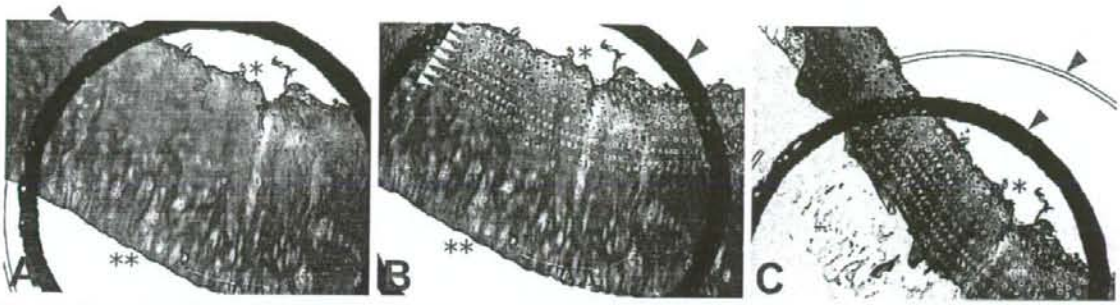

Figure 1. Separation and acquisition of cartilage zone by laser capture microdissection (LCM). **A,** A tissue section was set on an LCM device, and a transparent plastic film was placed on the section. Cartilage zones were identified through the film. **B,** The zone of interest was fixed to the film by shooting with a laser. The area was shot multiple times until the entire zone was anchored to the film. Arrays of spots indicated by **yellow arrowheads** are the laser shot marks. **C,** After laser shooting, any unnecessary area of the section was removed, and only the zone of interest that had adhered to the film was obtained. Acquisition of a middle cartilage zone from a section containing middle and deep zones is shown. The superficial zone of this section was already lost to disease. **Single** and **double asterisks** indicate the top and bottom of the section, respectively. Transparent and bold black arcs indicated by **blue arrowheads** are the marks on the plastic film. (Original magnification × 2.)

http://www.hosp.go.jp/~sagami/rinken/crc/index.html), and 72°C for 6 seconds.

The amount of specific cDNA was quantified with a standard curve based on the known amounts of PCR product. When SYBR Green I was used for monitoring, melting curves were routinely recorded to verify singularity of the product. A previous study showed that *GAPDH* is expressed at similar levels in chondrocytes in normal and OA cartilage (8). Consistently, the result of our preliminary experiment indicated that the expression of *GAPDH* and *ACTB* (a gene coding β-actin) was highly correlated in cartilage samples from OA and control knees. Thus, in this study, *GAPDH* was used as the internal standard for gene expression, and cDNA levels were expressed as the ratio of gene expression:*GAPDH* expression.

Statistical analysis. Pearson's correlation and paired *t*-tests were calculated with the SAS software package (SAS Institute, Cary, NC). For some data, statistical differences were determined by an analysis of variance followed by a Scheffe's post hoc test. *P* values less than 0.05 were considered significant.

RESULTS

Up-regulated expression of cartilage matrix molecules at different regional intensities in OA cartilage. In each OA joint, cartilage was harvested from femoral condyles, both from macroscopically intact areas and

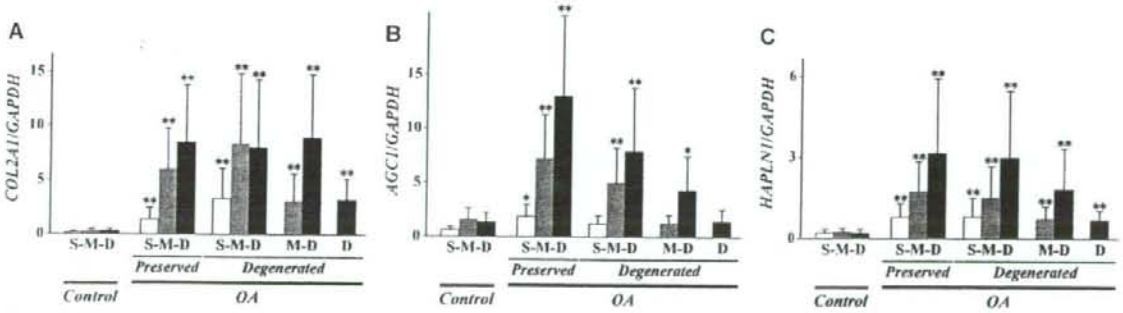

Figure 2. Expression of cartilage matrix genes in osteoarthritic (OA) and nonarthritic (control) cartilage. Cartilage samples obtained from nonarthritic knee joints and knee joints with end-stage OA were divided into superficial (S), middle (M), and deep (D) zones by laser capture microdissection, and expression of cartilage matrix genes was evaluated in the respective zones. In OA joints, cartilage samples were harvested from macroscopically intact areas (preserved) and areas with various degrees of cartilage degeneration (degenerated). The latter samples were divided into 3 groups (S-M-D, M-D, and D) according to the zones retained at the site. Expression of the genes coding type II collagen (*COL2A1*) (**A**), aggrecan (*AGC1*) (**B**), and link protein (*HAPLN1*) (**C**) is shown as ratios of the expression of *GAPDH*. Each bar represents the results from at least 16 samples. Values are the mean and SD. * = $P < 0.05$; ** = $P < 0.01$, versus the corresponding zone in control cartilage.

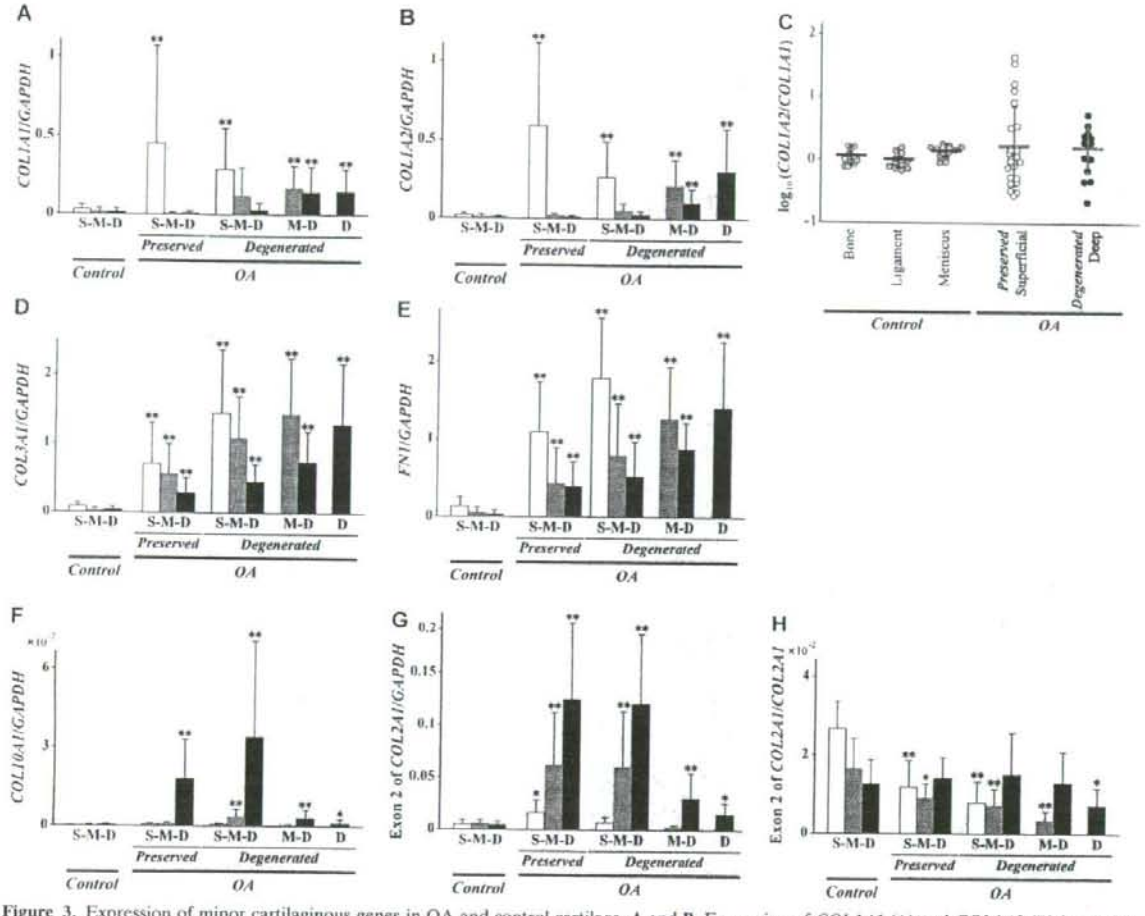

Figure 3. Expression of minor cartilaginous genes in OA and control cartilage. **A** and **B**, Expression of *COL1A1* (**A**) and *COL1A2* (**B**) in control and OA cartilage is shown as ratios of the expression of *GAPDH*, as described in Figure 2. **C**, The expression ratios of *COL1A2* to *COL1A1* were obtained in the superficial zone in preserved areas and in the deep zone in degenerated areas where the zone was directly exposed to the joint cavity, and were compared with those obtained in bone, ligaments, and menisci harvested from control joints. Ratios are shown in logarithmic values. **D–F**, Expression of genes coding type III collagen (*COL3A1*) (**D**), fibronectin (*FN1*) (**E**), and type X collagen (*COL10A1*) (**F**) is shown as ratios of the expression of *GAPDH*. **G** and **H**, Expression of exon 2 of *COL2A1* gene is shown as ratios of the expression of *GAPDH* (**G**) and by ratio to the total expression of *COL2A1* (**H**). S-M-D, M-D, and D under the respective groups of bars indicate the zone(s) retained in the samples. Each bar represents the results from at least 11 samples. Values are the mean ± SD. * = $P < 0.05$; ** = $P < 0.01$, versus the corresponding zone in control cartilage. See Figure 2 for definitions.

from areas showing macroscopic signs of degeneration. In this study, such areas were designated "preserved" and "degenerated" areas, respectively. OA and control cartilage samples were separated into 3 cartilage zones by LCM, and gene expression was evaluated in the respective cartilage zones by real-time PCR, considering the zonal difference and the severity of cartilage degeneration.

Compared with that in the control cartilage, the expression of type II collagen was strongly up-regulated in all areas in OA cartilage (Figure 2A). The up-regulation was most apparent in the deep zone, where the expression was ~20-fold that in the corresponding zone of the control cartilage. In contrast, the level of up-regulation was considerably reduced in the upper part of the degenerated cartilage. Where the zones were

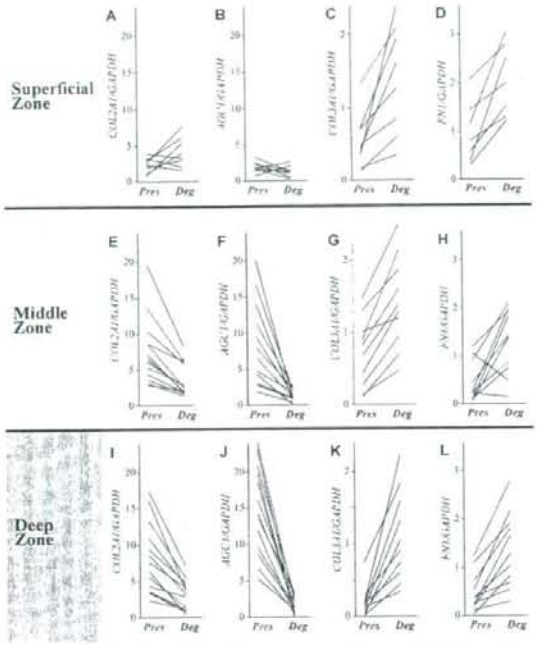

Figure 4. Comparison of gene expression between preserved (Pres) and degenerated (Deg) areas. In each osteoarthritic joint, the expression of 4 genes was compared in the respective cartilage zones between the preserved and degenerated areas. For the middle and deep zones, expression in the degenerated area was determined where the zones were directly exposed to the joint cavity due to the loss of the upper zone(s) to the disease. Expression of *COL2A1* (**A, E,** and **I**), *AGC1* (**B, F,** and **J**), *COL3A1* (**C, G,** and **K**), and *FN1* (**D, H,** and **L**) in the superficial, middle, and deep zones is shown. In these graphs, each line represents the expression in a single joint. Results from 7–13 joints are shown as the ratio of gene expression to *GAPDH* expression.

directly exposed to the joint cavity due to the loss of the upper zone(s) to the disease, the expression levels in the middle and deep zones were almost half of those in the preserved areas.

The expression of aggrecan was also enhanced in OA cartilage (Figure 2B). Similar to type II collagen, the increase was most obvious in the deep zone of the preserved area but was less intense in the degenerated area. In this gene, the regional change of expression was more obvious than that in type II collagen. Thus, in the middle and deep zones exposed to the joint cavity in degenerated areas, the expression was virtually unenhanced, and the expression levels were similar to those in the control cartilage. The expression of link protein presented a regional change similar to that of aggrecan, although the decline in the degenerated area was less apparent (Figure 2C).

Spatially distinctive patterns in OA cartilage shown by expression of minor cartilaginous genes induced by OA. In OA, there is enhanced expression of several genes that are not expressed at substantial levels in normal cartilage. Types I, III, and X collagen and fibronectin are among those genes (5,9,13,14,20–22), which are termed minor cartilaginous genes in this report. A change in alternative splicing also occurs in OA, and there is induced expression of exon 2 of type II collagen gene, which is not expressed in healthy adult cartilage (11,12). Therefore, we evaluated the expression of these genes and the exon in OA and control cartilage, paying special attention to regional differences.

In accordance with previous reports (6–8,23), the expression of type I collagen genes, *COL1A1* and *COL1A2*, was induced in OA cartilage (Figures 3A and

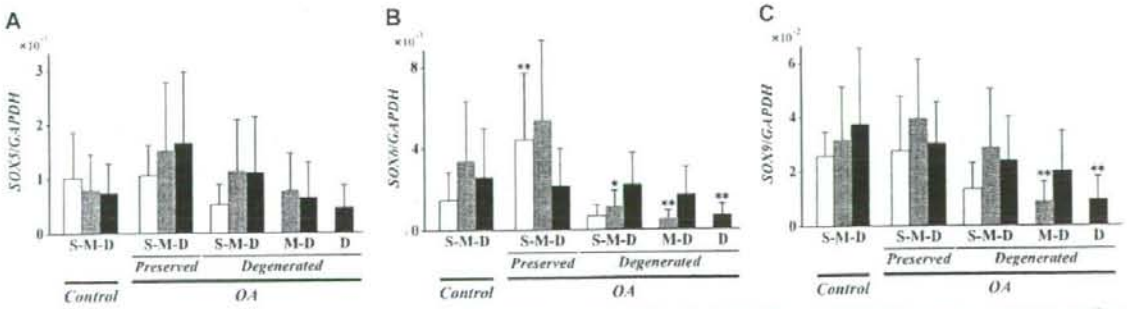

Figure 5. Expression of *SOX* genes in OA and control cartilage. Expression of *SOX5* (**A**), *SOX6* (**B**), and *SOX9* (**C**) in control and OA cartilage is shown as ratios of the expression of *GAPDH*, as described in Figure 2. S-M-D, M-D, and D under the respective groups of bars indicate the zone(s) retained in the samples. Each bar represents the results from at least 13 samples. Values are the mean and SD. * = $P < 0.05$; ** = $P < 0.01$, versus the corresponding zone in control cartilage. See Figure 2 for definitions.